RSC Advances

PAPER



Cite this: *RSC Adv.*, 2024, **14**, 28148

# TpBD/UiO-66-$NH_2$ micro–mesoporous hybrid material as a stationary phase for open tubular capillary electrochromatography†

Lidi Gao,[ab] Xinran Qu,[a] Shuang Meng,[a] Mo Chen,[a] Yuxin He,[a] Fuquan Zhao,[a] Hongtao Chu,[ab] Shili Qin *[ab] and Fenglong Jin*[c]

Received 15th July 2024
Accepted 21st August 2024

DOI: 10.1039/d4ra05097e

rsc.li/rsc-advances

The excellent stability of covalent organic frameworks (COFs) and the diversity of metal organic frameworks (MOFs) make MOF/COF hybrid materials promising candidates for chromatographic stationary phases. In this paper, a TpBD/UiO-66-$NH_2$ hybrid material was synthesized through a Schiff-base reaction between TpBD COFs and UiO-66-$NH_2$ MOFs; characterized using Fourier-transform infrared spectroscopy, X-ray diffraction, and X-ray photoelectron spectroscopy; and bonded to a capillary to prepare a TpBD/UiO-66-$NH_2$-bonded open tubular capillary electrochromatography (OT-CEC) column. Results suggested that the hybrid material had the crystal morphology of a single COF and MOF, a micro–mesoporous structure, and good thermal stability. The inner surface of the OT-CEC column was tightly and uniformly distributed with the stationary phase (~1.5 μm). The baseline separation of 13 amino acids and three families (4 acidic antibiotics, 4 preservatives and 6 sulfonamides) of emerging pollutant mixtures was achieved due to the synergistic effect of TpBD and UiO-66-$NH_2$ in the stationary phase. The OT-CEC column showed good reproducibility and stability with relative standard deviations of migration time and resolutions in the range of 1.17–3.93% and 1.79–4.31%, respectively.

## 1 Introduction

Separation of many complex components with similar structures or properties in a sample is one of the frontiers of analytical chemistry.[1] The abuse of emerging pollutants such as antibiotics and preservatives has caused a large number of pollutants to be released into the environment, which poses a threat to human beings and various other organisms.[2,3] At present, although there are many methods for detecting emerging pollutants, including enzyme-linked immunosorbent assay (ELISA), gas chromatography-mass spectrometry (GC-MS), high performance liquid chromatography (HPLC), liquid chromatography-mass spectrometry (LC-MS), capillary electrophoresis (CE) and capillary electrochromatography (CEC),[4–6] it is rare and challenging to establish a simple, rapid and universal simultaneous separation method for complex emerging pollutants.

CEC has a stationary phase to retain and distribute analytes and an electroosmotic flow (EOF) driven by an electric field, resulting in high selectivity, high efficiency and low sample consumption,[7] and its application is becoming increasingly widespread in the domains of separation and analysis. In particular, open tubular CEC (OT-CEC) has been widely employed due to its advantages of simple preparation, low back pressure and no bubble generation. However, disadvantages of a low phase ratio and low column capacity hinder its wide application.[8,9] Therefore, the development of new porous OT-CEC stationary phases with good stability and many active sites becomes an optimal solution.

Porous organic framework materials, such as covalent organic frameworks (COFs) or metal organic frameworks (MOFs), have been used as stationary phases for OT-CEC and demonstrate good separation performance due to their large specific surface area, rich and adjustable pore environments and many active sites from organic ligands and/or unsaturated metal centers.[8,9] However, it is not easy to select suitable MOFs to construct the stationary phase of OT-CEC because most MOFs will collapse in aqueous solution or upon contact with certain solvents.[10] Although a few MOFs exhibit adequate stability, their active sites are insufficient for the effective separation of complex systems.[11] In contrast, COFs themselves generally supply enough active sites such as –OH, –CHO, and –COOH or through easy surface modification, and their stability is strong, even stronger than that of some MOFs with higher

[a]College of Chemistry and Chemical Engineering, Qiqihar University, Qiqihar 161006, China. E-mail: qinshili1103@163.com

[b]Heilongjiang Industrial Hemp Processing Technology Innovation Center, Qiqihar University, Qiqihar 161006, China

[c]Technology Innovation Center of Industrial Hemp for State Market Regulation, Qiqihar University, Qiqihar 161006, China

† Electronic supplementary information (ESI) available. See DOI: https://doi.org/10.1039/d4ra05097e

stability.[12] However, the crystallinity of COFs is somewhat inferior to that of MOFs.

Therefore, the crystal structure of COFs should be improved to enhance the stability of MOFs *via* the construction of MOF/COF hybrid material and obtain various excellent performances (Fig. 1).[13,14] In 2016, Fu *et al.*[15] first reported that ZIF-8 MOF was grown on COF-300 to prepare hybrid material membranes, which demonstrated higher separation selectivity for $H_2/CO_2$ than the original individual MOF or COF membranes. Wang's research group[16,17] studied cotton fiber and corncob functionalized by UiO-66-$NH_2$ MOF@TpBD COF as extractant and adsorbent for the removal of bisphenols from water samples and enhancing the adsorption of sulfonamides and its metabolites, respectively. Both showed good adsorption capacity. Recently, Pang *et al.*[18] developed the core–shell MOF@COF ($NH_2$-UiO-66@TpBD-COF) hybrids. The hybrids showed superior catalytic performance in the visible light-driven oxidative coupling of amines to imines in air. However, to date, there have been no reports on the use of MOF/COF hybrid materials as a stationary phase for CEC.

TpBD COF, as an imine COF, has the excellent characteristics of good chemical stability, easy modification, –$NH_2$, –OH, –CHO active groups as well as good separation performance.[19,20] The high specific surface area, excellent crystallization performance, good porosity and unsaturated metal sites of UiO-66-$NH_2$ play important roles in adsorption and separation.[16–18,21] The TpBD/UiO-66-$NH_2$ hybrid material will demonstrate excellent separation performance and wide application range as the stationary phase due to their synergistic effect, such as more active sites, high specific surface area and hierarchical pore structure in CEC. In this paper, TpBD/UiO-66-$NH_2$ hybrid material was synthesized through the Schiff-base reaction between TpBD COF and UiO-66-$NH_2$ MOF. TpBD/UiO-66-$NH_2$-bonded OT-CEC column was prepared using TpBD/UiO-66-$NH_2$ hybrid material as the stationary phase for the first time and was applied for the simultaneous separation of 13 amino acids and three families (4 acidic antibiotics, 4 neutral preservatives and 6 amphoteric sulfonamides) of emerging pollutant mixtures.

## 2 Materials and methods

### 2.1 Chemicals and materials

Phloroglucinol (Tp), benzidine (BD), 3-aminopropyltriethoxysilane (APTES) and glutaraldehyde (50%) (v/v) were purchased from Aladdin Industrial Co. (Shanghai, China). 50% glutaraldehyde was diluted with ultrapure water (18.2 MΩ cm) and adjusted by 1 mol $L^{-1}$ NaOH solution to obtain a glutaraldehyde solution (2%) (v/v) with pH = 11. Anhydrous zirconium chloride ($ZrCl_4$) and 2-aminoterephthalic acid (BDC-$NH_2$) were obtained from Beijing InnoChem Science & Technology Co., Ltd (Beijing, China). Glacial acetic acid, thiourea, benzene, toluene and *o*-xylene were purchased from Tianjin Kemiou Reagent Co., Ltd (Tianjin, China). Amino acids (glutamic acid (Glu), aspartic acid (Asp), serine (Ser), alanine (Ala), valine (Val), threonine (Thr), isoleucine (Ile), leucine (Leu), methionine (Met), tryptophan (Trp) and phenylalanine (Phe), arginine (Arg) and histidine (His)) were obtained from Sinopharm Chemical Reagent Ltd (Shanghai, China). Preservatives (methyl-4-hydroxybenzoate (MHB), ethyl-4-hydroxybenzoate (EHB), propyl-4-hydroxybenzoate (PHB), butyl-4-hydroxybenzoate (BHB)) were ordered from Jiuding Chemical Co. (Shanghai, China). Sulfonamides (sulfamerazine (SM1), sulfadimethoxine (SDM), sulfamethazine (SM2), sulfamethoxazole (SMZ), sulfisoxazole (SIZ), sulfathiazole (ST)) and acidic antibiotics (metronidazole (Mnz), chloramphenicol (Cpl), tetracycline hydrochloride (Tet), chlortetracycline hydrochloride (Ctc)) were purchased from the National Institute for the Control of Pharmaceutical and Biological Products (Beijing, China) (Fig. S1†). The solvents used in CEC were chromatographic grade. Fused silica capillaries (75 μm i.d. and 375 μm o.d.) were from Yongnian Fiber Factory (Handan, China).

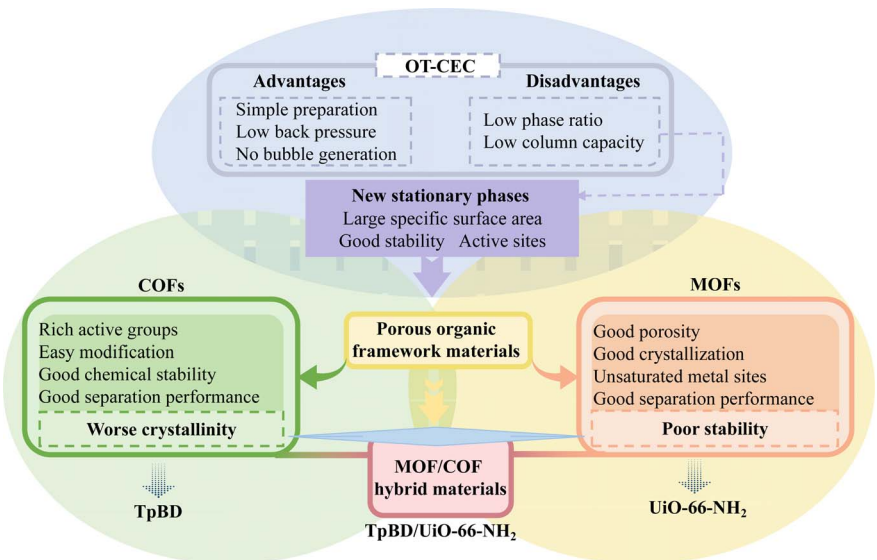


Fig. 1 A schematic of the research route.

### 2.2 Instruments

All CEC separations were conducted on a CE system equipped with a diode array detector (Agilent 7100, Waldbronn, Germany). The surface morphology and elemental distribution were done by an S-4300 scanning electron microscope (SEM) equipped with an energy-dispersive X-ray spectrometer (EDS) (Hitachi, Japan). The morphology of TpBD/UiO-66-$NH_2$ was also observed by an H-7650 transmission electron microscope (TEM) (Hitachi, Japan). X-ray photoelectron spectroscopy (XPS) characterization was performed using an ESCALAB 250 photoelectron spectrometer (ThermoFisher Scientific, USA). Fourier-transform infrared (FT-IR) spectra were obtained by an FT-IR spectrometer (Spectra PE Co, USA). X-ray diffraction (XRD) spectra were collected with a Bruker D8 diffraction instrument (Karlsruhe, Germany). Nitrogen adsorption/desorption isotherms were examined on a surface area analyzer (Micromeritics ASAP, USA). Thermogravimetric (TG) measurement was performed using an STA 449F5 (Netzsch, Germany) device. The zeta potential was measured with a Nano ZS 90 zeta potential analyzer (Malvern, UK).

### 2.3 Preparation of TpBD/UiO-66-$NH_2$-bonded OT-CEC column

The TpBD/UiO-66-$NH_2$-bonded OT-CEC column was obtained by modifying UiO-66-$NH_2$ to the TpBD-bonded OT-CEC column. The column preparation followed a four-step process: (i) pretreatment of the capillary column, (ii) activation of aldehyde groups, (iii) linkage of TpBD according to our previous report,[20] as well as (iv) modification of UiO-66-$NH_2$. In the last step, 38.8 mg UiO-66-$NH_2$ was dispersed in 4 mL DMF, then the suspension was filled into the TpBD-bonded OT-CEC column, which was maintained in a water bath at 80 °C for 24 h by sealing both the ends. The modification procedure was repeated two times (Fig. 2). The OT-CEC column was flush with DMF and methanol to remove the unreacted substances in the capillary. The TpBD/UiO-66-$NH_2$-bonded OT-CEC columns were obtained.

### 2.4 Synthesis of TpBD/UiO-66-$NH_2$

TpBD/UiO-66-$NH_2$ was synthesized by the solvothermal method for FT-IR, XRD, SEM, EDS, XPS, TEM, TG, nitrogen adsorption/desorption and zeta-potential characterization or determination as the stationary phase of the TpBD/UiO-66-$NH_2$-bonded OT-CEC column. TpBD and UiO-66-$NH_2$ were synthesized according to the previous reports with minor modification, and their hybridization synthesis is represented in Fig. S2.†[21,22] 27.8 mg TpBD was dissolved in 20 mL DMF, in which 38.8 mg UiO-66-$NH_2$ was added. The mixture was refluxed for 6 h at 80 °C under nitrogen atmosphere.[22,23] The resultant product was centrifuged, after which the clear supernatant was decanted. Subsequently, the precipitate, TpBD/UiO-66-$NH_2$, was sequentially washed three times with DMF and methanol and finally dried at 60 °C for 12 h in vacuum.

### 2.5 CEC conditions

The total length of the as-prepared TpBD/UiO-66-$NH_2$-bonded OT-CEC column was 40.0 cm, and the effective length was 26.5 cm. The ammonium acetate buffer with a pH range of 6.0 to 10.0 was chosen for detection. All the sample solutions were filtered by a 0.45 μm filter membrane. The injection pressure was 50 mbar × 3 s, and the instrument was operated at room temperature (no more than 25 °C).

## 3 Results and discussion

### 3.1 Preparation conditions for the TpBD/UiO-66-$NH_2$-bonded OT-CEC column

To achieve the strong synergistic effect and optimal separation performance, it was significantly important to obtain the optimal bonding amount of UiO-66-$NH_2$ in the stationary phase under the condition of maintaining the crystallinity of TpBD and UiO-66-$NH_2$. Based on our previous study,[20] the main influence factors of UiO-66-$NH_2$ bonded to TpBD-bonded OT-CEC column were investigated including reaction temperature, reaction time and UiO-66-$NH_2$ dosage by the orthogonal test (Table 1). Column efficiency was used as the evaluation index with benzene as the analyte.

The data showed that the UiO-66-$NH_2$ dosage, reaction temperature and reaction time all had a significant effect on the column efficiency, and the influence intensity was in the order UiO-66-$NH_2$ dosage > reaction temperature > reaction time ($R_C$ > $R_A$ > $R_B$). The maximum column efficiency (37 745 plates per m) was achieved under the conditions of reacting for 24 h at 80 °C

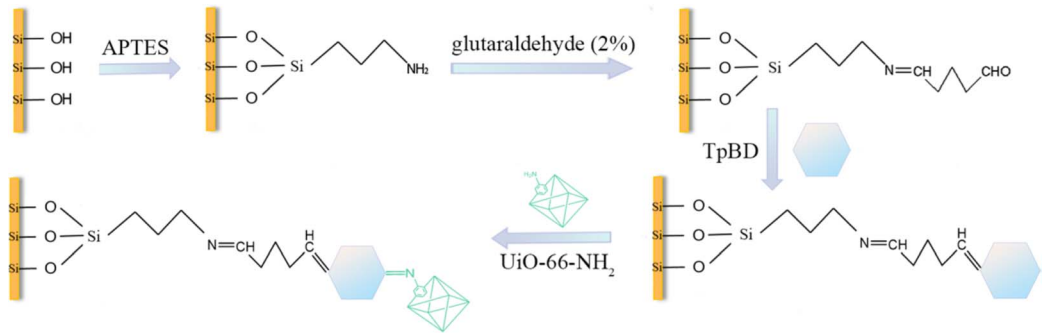


Fig. 2 Preparation scheme for the TpBD/UiO-66-$NH_2$-bonded OT-CEC column.

Table 1 Optimization of the preparation conditions of the TpBD/UiO-66-$NH_2$-bonded OT-CEC column

| Experiment no. | Factors | | | Column efficiency (plates per m) |
|---|---|---|---|---|
| | Reaction temperature (°C) | Reaction time (h) | UiO-66-$NH_2$ dosage (mg) | |
| | A | B | C | |
| 1 | 60 | 12 | 12.9 | 26 904 |
| 2 | 60 | 24 | 25.9 | 28 560 |
| 3 | 60 | 48 | 38.8 | 32 639 |
| 4 | 80 | 12 | 25.9 | 33 779 |
| 5 | 80 | 24 | 38.8 | 37 745 |
| 6 | 80 | 48 | 12.9 | 28 187 |
| 7 | 100 | 12 | 38.8 | 30 401 |
| 8 | 100 | 24 | 12.9 | 28 190 |
| 9 | 100 | 48 | 25.9 | 29 611 |
| $T_{1j}$ | 88 103 | 91 084 | 83 291 | |
| $T_{2j}$ | 99 711 | 96 706 | 91 950 | |
| $T_{3j}$ | 88 202 | 90 437 | 100 785 | |
| $R_j$ | 11 608 | 6269 | 17 494 | |

with 38.8 mg UiO-66-$NH_2$ (experiment no. 5). Meanwhile, the stationary phases of the MOF/COF hybrid materials containing three different dosages of UiO-66-$NH_2$ were characterized by XRD. As shown in Fig. 3, the hybrid materials contained a strong characteristic diffraction peak of TpBD COF at 3.3°, indicating the existence of TpBD COF with its original crystal structure in the hybrid materials.[24] The diffraction peaks at 7.36° and 8.50° proved that UiO-66-$NH_2$ was successfully introduced into the hybrid materials.[25] However, the position of the diffraction peaks in the hybrid materials, such as 25.68° and 30.66°, slightly changed compared with that of UiO-66-$NH_2$, and their intensity and sharpness all reduced, probably because the bonding of TpBD and UiO-66-$NH_2$ led to their poor crystallinity. Furthermore, the diffraction peaks of UiO-66-$NH_2$ in the hybrid materials became strong with the increasing UiO-66-$NH_2$ dosage. However, when exceeding 38.8 mg UiO-66-$NH_2$, the viscosity of the suspension was too large to be poured into the capillary column. Therefore, the optimal preparation conditions selected were same as that of experiment no. 5.

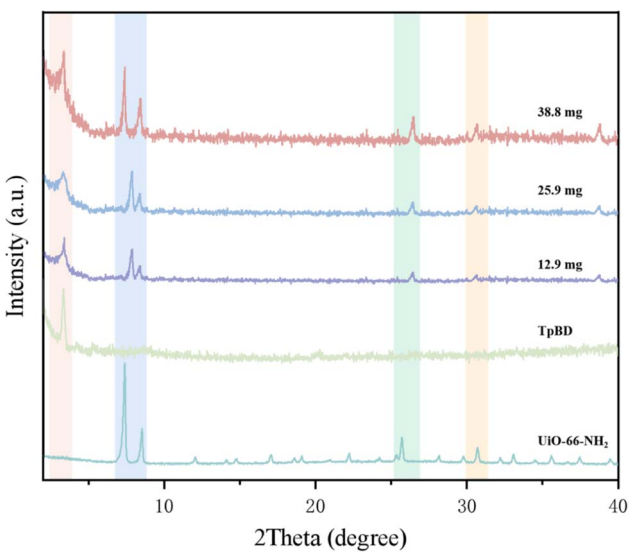


Fig. 3 XRD spectra of TpBD/UiO-66-$NH_2$ (experimental conditions: TpBD dosage, 27.8 mg; reaction temperature, 80 °C; reaction time, 24 h), TpBD and UiO-66-$NH_2$.

### 3.2 Characterization of TpBD/UiO-66-$NH_2$

Fig. 4 shows the FT-IR spectra of TpBD, UiO-66-$NH_2$ and TpBD/UiO-66-$NH_2$. TpBD/UiO-66-$NH_2$ contained almost all of the characteristic absorption peaks from UiO-66-$NH_2$ and TpBD. The Zr–O–Zr bending vibration peak was at 764 $cm^{-1}$. The N–H symmetric and antisymmetric stretching vibration peaks in the amino groups were at 3364 $cm^{-1}$ and 3452 $cm^{-1}$ corresponding to the peaks at 3361 $cm^{-1}$ and 3453 $cm^{-1}$ of UiO-66-$NH_2$. The C–N stretching vibration bands in the range of 1260–1280 $cm^{-1}$ corresponded to the bands at 1250 $cm^{-1}$ of UiO-66-$NH_2$ and 1283 $cm^{-1}$ of TpBD. The symmetric and antisymmetric stretching vibration peaks of carboxyl groups in the BDC-$NH_2$ ligand appeared at 1390 $cm^{-1}$ and 1450 $cm^{-1}$, which were red-shifted from the peaks at 1380 $cm^{-1}$ and 1430 $cm^{-1}$ for UiO-66-

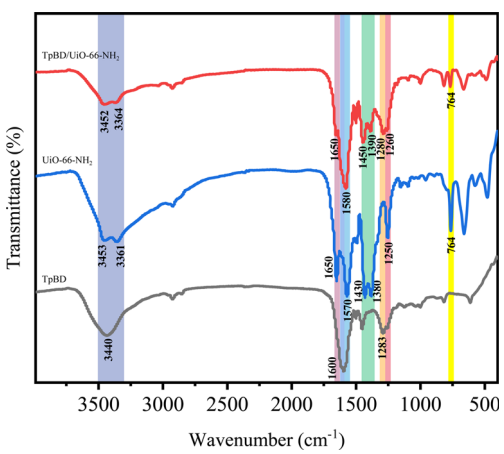


Fig. 4 FT-IR spectra of TpBD, UiO-66-$NH_2$, and TpBD/UiO-66-$NH_2$.

$NH_2$.[26,27] In addition, the wider absorption band in the range of 1580–1650 $cm^{-1}$ indicated the overlapping vibration peaks of C=N, C=O and C=C of the benzene ring skeleton in TpBD and the reaction between –COOH in the ligand and $Zr^{4+}$ in UiO-66-$NH_2$.[28] Although most of the absorption displacements were slightly changed compared with TpBD and UiO-66-$NH_2$, they confirmed the successful synthesis of the TpBD/UiO-66-$NH_2$ hybrid material.

The stacking and overlapping of spherical TpBD and octahedral UiO-66-$NH_2$ are observed in Fig. 5A and B. The chemical composition of TpBD/UiO-66-$NH_2$ was determined by EDS elemental mapping (Fig. S3A–D).† The results showed that there were uniformly distributed O, C, N and Zr elements on the hybrid material, which further proved that the interaction between TpBD and UiO-66-$NH_2$ was chemical bonding.

The elemental composition and chemical state of TpBD/UiO-66-$NH_2$ were analyzed by XPS (Fig. 6). The full-scan spectrum of TpBD/UiO-66-$NH_2$ indicated the presence of carbon (C), nitrogen (N), oxygen (O) and zirconium (Zr) in TpBD/UiO-66-$NH_2$ (Fig. 6A), which was in line with the EDS elemental mapping results. The high-resolution spectra of the deconvoluted C 1s and N 1s (Fig. 6B and C) displayed the characteristic energy peaks of TpBD[29] and that of deconvoluted Zr 3d as proof of the existence of UiO-66-$NH_2$ in TpBD/UiO-66-$NH_2$ was shown in Fig. 6D.[17]

The C 1s spectrum of TpBD/UiO-66-$NH_2$ was divided into five peaks corresponding to C=O (287.19 eV), C=N (285.59 eV), C–N (284.80 eV), C=C (283.93 eV) and C–C (283.18 eV), respectively. Among them, the binding energy of C=N of the hybrid material was not much different from that in TpBD because the C=N of both was produced by the Schiff base reaction. The positive binding energy shift of C=O (+0.74 eV) was due to the introduction of additional C=O of carboxyl groups from UiO-66-$NH_2$.

The N 1s spectrum of TpBD/UiO-66-$NH_2$ was composed of two peaks, N=C and N–C. The binding energy of N–C (397.91 eV) was obviously lowered by 1.61 eV and 0.37 eV compared with those of TpBD (399.52 eV) and UiO-66-$NH_2$ (398.28 eV), which suggested that there was chemical bonding between the aldehyde groups from Tp in TpBD and the amino groups in UiO-66-$NH_2$.[30] The results further indicated that UiO-66-$NH_2$ was successfully bonded to TpBD. In addition, the bonding ratio of each TpBD six-membered ring to the UiO-66-$NH_2$ octahedral unit was about 5 : 1 in TpBD/UiO-66-$NH_2$, according to the calculation of the XPS data (Table S1†).[31]

TpBD/UiO-66-$NH_2$ had a large specific surface area (340.04 $m^2$ $g^{-1}$) and exhibited structural characteristics of the micropores and mesopores (the main pore size of 1.18–2.65 nm) due to the hybrid formation of TpBD with mesopores and UiO-66-$NH_2$ with micropores[32,33] (Fig. 7), which could provide more active sites for the small molecular analytes. The specific surface area and average pore volume of TpBD/UiO-66-$NH_2$ were smaller than those of TpBD or UiO-66-$NH_2$, indicating that partly intersected pore channels might exist (Table S2†).

The thermal stability of TpBD/UiO-66-$NH_2$ was evaluated by the TGA curve (Fig. 8). When the temperature was raised to 113.2–204.6 °C, the weight loss was due to the presence of solvents (water, DMF and methanol) adsorbed on the surface of the material. The weight loss at 204.6–419.8 °C was mainly from the dehydroxylation of $Zr_6$ clusters in the hybrid material.[34] The rapid decomposition of various ligands of TpBD/UiO-66-$NH_2$ contributed to the weight loss after 419.8 °C.[34,35] Only $ZrO_2$ was left when the hybrid material was heated to 800.4 °C. The results showed that the hybrid material had good thermal stability and could be used as the stationary phase of the OT-CEC column.

Zeta potential can reflect the surface charge of TpBD/UiO-66-$NH_2$, which is very important for analyzing the separation mechanism. The change in the zeta potential with pH values indicated that the surface of TpBD/UiO-66-$NH_2$ was negatively charged (Fig. S4†). Although a small amount of amino groups existed in the form of $NH_3^+$ under acidic conditions, the dissociation of the large amount of Zr–OH into Zr–$O^-$ made the surface of TpBD/UiO-66-$NH_2$ negatively charged. There were more negative charges with increasing pH, which was mainly attributed to the ionization of carboxyl groups from UiO-66-$NH_2$ and phenolic hydroxyl groups from the TpBD of TpBD/UiO-66-$NH_2$ in sequence.

### 3.3 Characterization of TpBD/UiO-66-$NH_2$-bonded OT-CEC column

Compared with the bare capillary column (Fig. 9A), it was observed that the stationary phase (~1.5 μm) was tightly and uniformly distributed in the TpBD/UiO-66-$NH_2$-bonded OT-CEC column (Fig. 9B and C), which proved that TpBD/UiO-66-$NH_2$ was successfully bonded to the inner wall of the capillary.

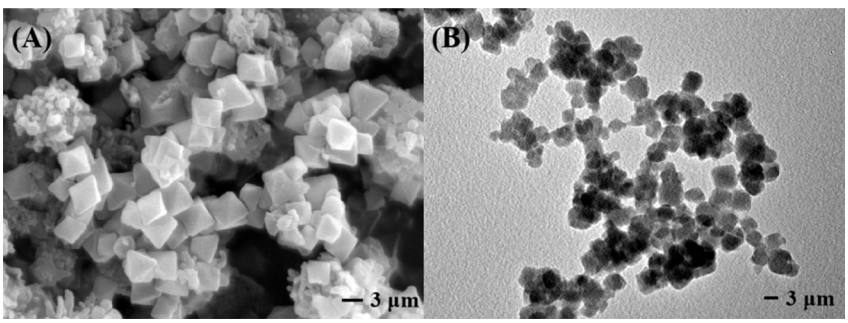


Fig. 5 SEM (A) and TEM (B) images of TpBD/UiO-66-$NH_2$.

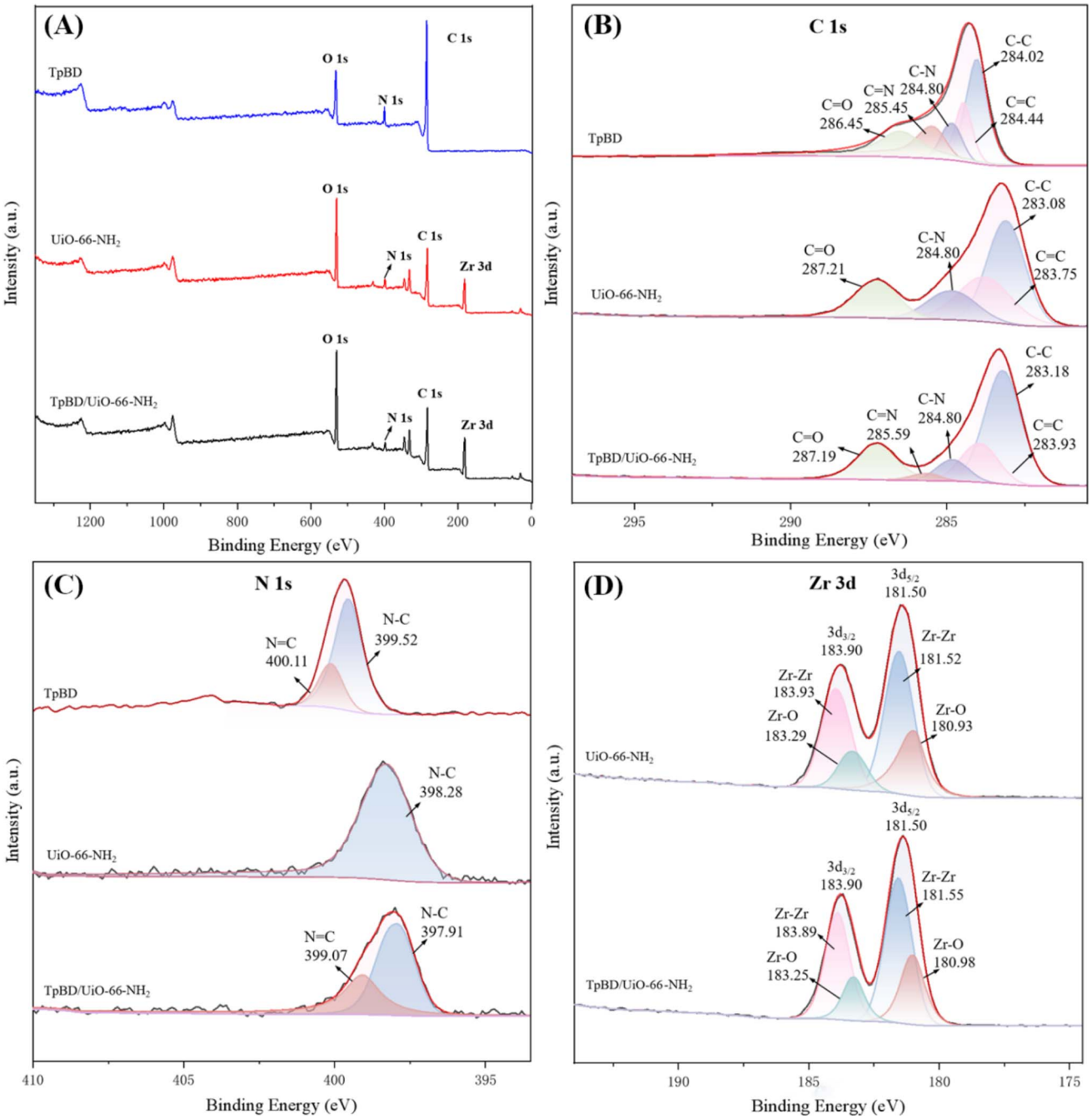


Fig. 6 XPS curves (A), high resolution C 1s (B), N 1s (C) and Zr 3d (D) XPS spectra of TpBD, UiO-66-$NH_2$ and TpBD/UiO-66-$NH_2$.

Spherical-like TpBD, octahedral UiO-66-$NH_2$ as well as their overlapping were clearly visible (Fig. 9D); however, their size was smaller than that of the TpBD/UiO-66-$NH_2$ hybrid material (Fig. 5), likely due to the microenvironment in the capillary. It was anticipated that these hybrid crystal structures would effectively improve the separation performance of the OT-CEC column.

### 3.4 EOF

EOF is the essential driving force for the separation process of the CEC method. The EOF of the TpBD/UiO-66-$NH_2$-bonded OT-CEC column was investigated in the buffer pH range of 4.0–10.0 using thiourea as a neutral marker (Fig. S5†). EOF increased with the increase in the pH values, maintaining the same direction as that observed in the bare capillary column, which were due to the negative surface charges of the stationary phase in the TpBD/UiO-66-$NH_2$-bonded OT-CEC column. However, the EOF of the TpBD/UiO-66-$NH_2$-bonded OT-CEC column was smaller than that of the bare capillary column at the same pH. The reason may be that the dissociation of Zr–OH, carboxyl groups and phenolic hydroxyl groups of EOF produced in the bonded column was weaker than that of the silanol groups in

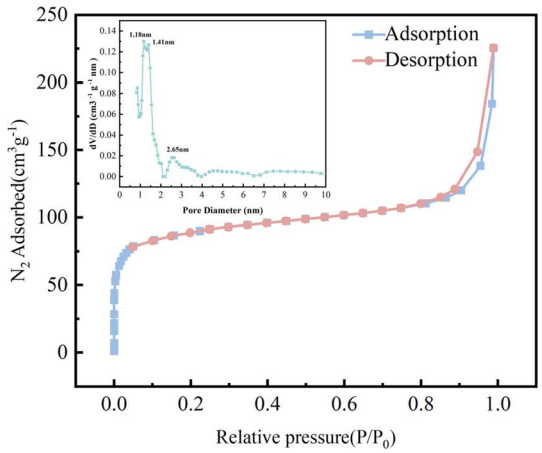


Fig. 7 $N_2$ adsorption–desorption isotherms of TpBD/UiO-66-$NH_2$ at 77.3 K ((inset): pore size distribution).

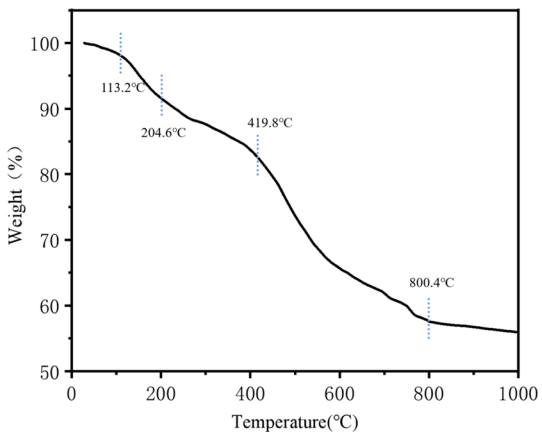


Fig. 8 TG curve of TpBD/UiO-66-$NH_2$.

the bare capillary column. However, the appropriate decrease in the EOF can increase the retention time of the analyte in the column and enhance the interaction between the analyte and the stationary phase to improve the separation efficiency.

### 3.5 Reproducibility and stability

The reproducibility and stability of the TpBD/UiO-66-$NH_2$-bonded OT-CEC column were evaluated using MHB, EHB, PHB, and BHB as the model analytes. Fig. S6† shows the chromatograms of MHB, EHB, PHB, and BHB after 1, 100 and 200 runs. It can be seen that there was no significant change in the migration time and peak shape after 200 runs. The relative standard deviations (RSDs) of the migration time for intra-day, inter-day and inter-column were 1.17–3.93%, and those of their resolutions were 1.79–4.31%, respectively (Table S3†). The results showed that the bonded OT-CEC column had good stability and satisfactory reproducibility.

### 3.6 Separation performance of the TpBD/UiO-66-$NH_2$-bonded OT-CEC column

The separation performance of the TpBD/UiO-66-$NH_2$-bonded OT-CEC column was investigated using 13 amino acids as template analytes, including 2 acidic (Glu and Asp), 9 neutral (Ser, Ala, Val, Thr, Ile, Leu, Met, Trp and Phe) and 2 basic (Arg and His) amino acids. Under the optimal separation conditions (Fig. S7A–C†), the simultaneous baseline separation of 13 amino acids was achieved within 8.1 min with $R_s = 1.63$–$10.35$ and separation factor ($\alpha$) = 1.06–1.35 (Fig. 10A and Table 2).

The separation of the 13 amino acids was mainly dependent on their pI values. Briefly, the basic amino acids like Arg were firstly eluted, followed by the neutral amino acids, and the last elution was that of the acidic Glu and Asp, which was consistent with the migration rule of the analytes in the CEC separation system (*i.e.*, cation > neutral molecule > anion) because Arg had

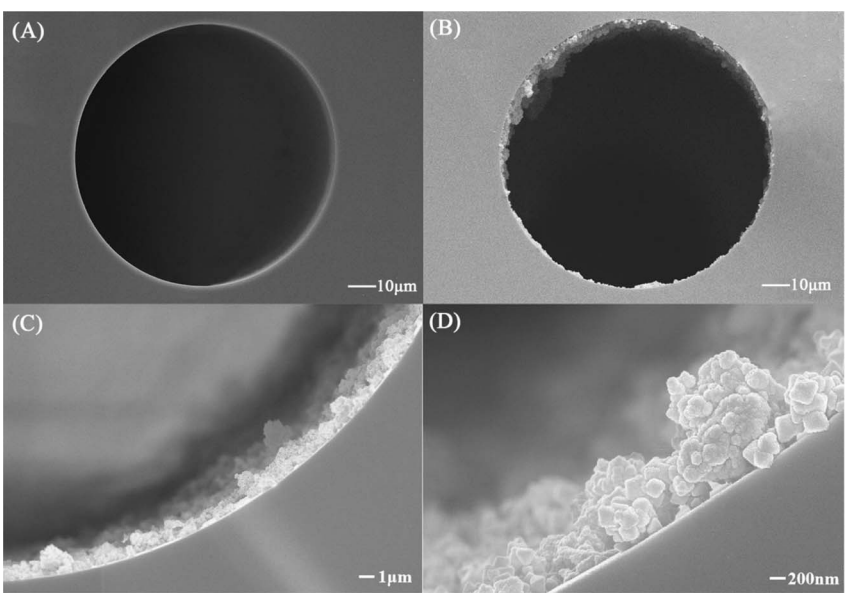


Fig. 9 SEM images of the cross section of the bare capillary column (A) and the TpBD/UiO-66-$NH_2$-bonded OT-CEC column (B–D).

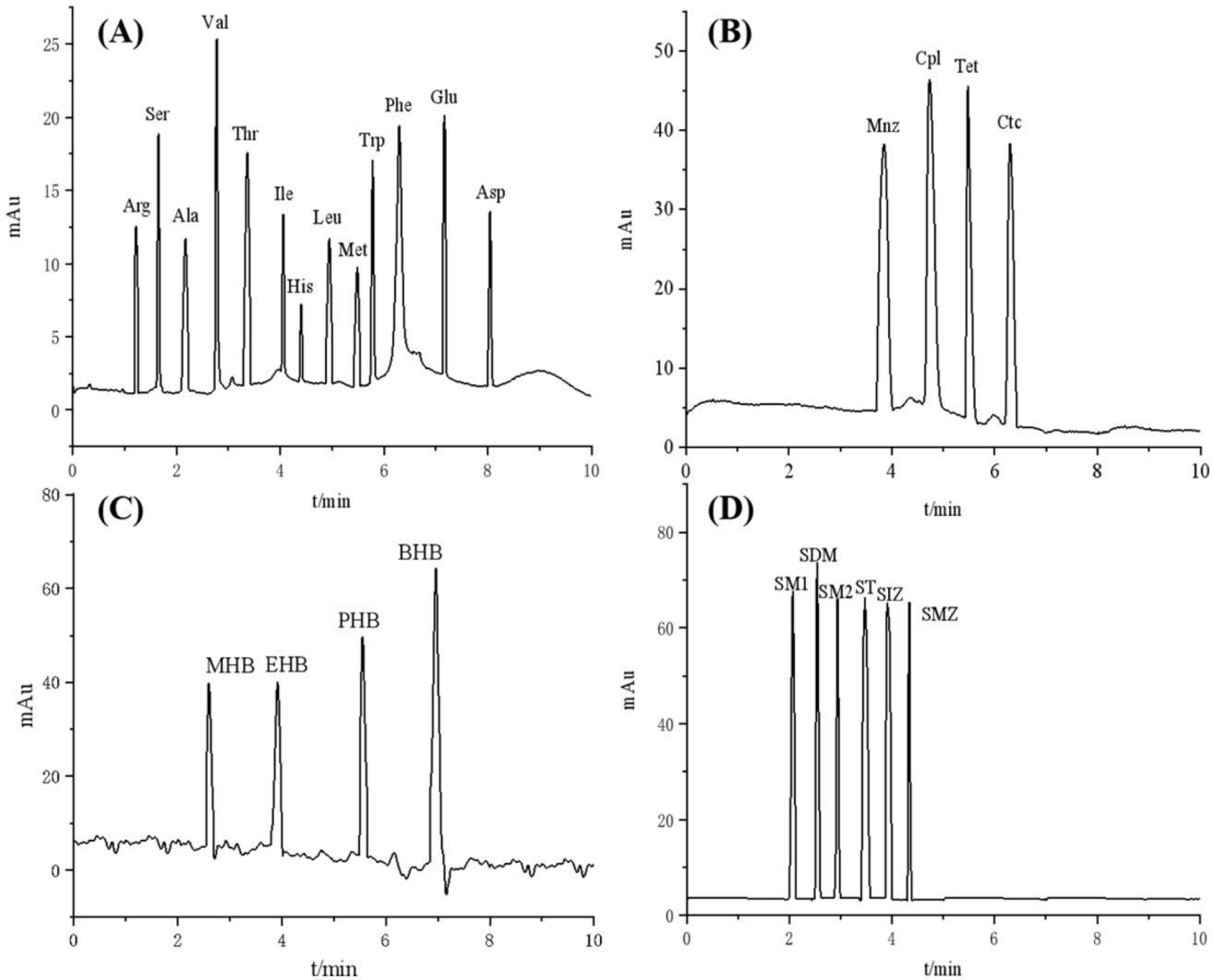


Fig. 10 Separation chromatogram of 13 amino acids (A), 4 antibiotics (B), 4 preservatives (C) and 6 sulfonamides (D) on the TpBD/UiO-66-$NH_2$-bonded OT-CEC column under optimized CEC conditions (experimental conditions: 20 mmol $L^{-1}$ of ammonium acetate buffer; pH = 8 for amino acids, pH = 9 for the other analytes; operating voltage, 15 kV; detection wavelength, amino acids at 214 nm, sulfonamides at 254 nm, and others at 270 nm.).

positive charge (pI > pH), neutral amino acids had slight negative charge (pI < pH) and the acidic ones (pI << pH) were highly negatively charged at the optimal pH 8. The retention time of His with the part negative charge (pI < pH) was similar to those of the neutral ones, although it is a basic amino acid. In addition, π–π interaction between the imidazole ring of His and the benzene ring of the ligands from TpBD and UiO-66-$NH_2$ in the stationary phase also prolonged its retention time. The same mechanism also clarified the last elution of Trp and Phe with the benzene ring as the neutral amino acids. The other neutral ones with polar (Ser and Thr) or nonpolar (Ala, Val, Ile, Leu, Met) side chains migrated according to the size of the side chain, from small to large. It was noticeable that Ile and Leu were isomers; their complete separation should be attributed to the steric hindrance effect between the analytes and the COF and MOF with the micro–mesoporous structures in the stationary phase.

In the case of the acidic antibiotics, the preservatives and the sulfonamides investigated, three families of the analytes simultaneously reached base-line separation under the broad CEC experimental conditions with buffer pH values of 8–10, buffer concentration of 20–25 mmol $L^{-1}$ and separation voltage of 15–20 kV (Fig. S8–S10†), and there was very short analysis time of 4.38 min for the sulfonamides. The separation mechanism including hydrogen bond, π–π interaction, molecular sieve effect, electrophoretic mobility, and dipole–dipole interaction between the analytes and the COF and/or MOF in the stationary phase played dominant roles in their separation.

For the acidic antibiotics, their migration order was Mnz, Cpl, Tet and Ctc, which was mainly attributed to the molecular sieve effect of the TpBD/UiO-66-$NH_2$ hybrid material with hierarchical pore structures, *i.e.*, the migration time of the analyte was shorter with the smaller molecular mass (Fig. 10B). In addition, it was noticeable that the longest retention time for

Table 2 Information and separation results for the analytes

| Analytes | pI or p$K_a$ (p$K_{a_1}$/p$K_{a_2}$) | Molecular volume[a] (Å$^3$) | Property | Log $P$ | Molecular mass | Optimal pH | $R_s$ | $\alpha$ |
|---|---|---|---|---|---|---|---|---|
| Arg | 10.76 (2.17/9.67) | 5.7 × 7.5 × 10.3 | Basic polar | −4.50 | 174.20 | 8 | — | — |
| His | 7.59 (2.49/9.04) | 5.7 × 7.0 × 6.9 | | −3.20 | 155.16 | | 4.11 | 1.09 |
| Ser | 5.68 (1.14/9.43) | 4.9 × 6.4 × 7.5 | Neutral polar | −0.80 | 105.09 | | 5.77 | 1.35 |
| Thr | 6.16 (2.19/9.36) | 5.3 × 6.0 × 7.6 | | −0.70 | 119.12 | | 3.41 | 1.21 |
| Ala | 6.00 (2.19/9.67) | 6.9 × 5.7 × 5.1 | Neutral nonpolar | 1.80 | 89.09 | | 4.97 | 1.32 |
| Val | 5.96 (2.32/9.61) | 7.5 × 6.3 × 5.6 | | 4.20 | 117.15 | | 3.41 | 1.28 |
| Ile | 6.02 (2.41/10.22) | 9.1 × 6.3 × 5.8 | | 4.50 | 131.17 | | 6.71 | 1.21 |
| Leu | 5.98 (2.28/9.82) | 9.2 × 6.9 × 5.3 | | 3.80 | 131.18 | | 4.85 | 1.12 |
| Met | 5.74 (2.25/10.06) | 5.0 × 7.1 × 10.8 | | 1.90 | 149.21 | | 3.79 | 1.11 |
| Trp | 5.89 (2.09/10.01) | 13.0 × 7.9 × 4.7 | | −0.90 | 204.23 | | 2.14 | 1.06 |
| Phe | 5.48 (2.09/10.43) | 11.3 × 6.9 × 5.3 | | 2.80 | 165.19 | | 1.63 | 1.09 |
| Glu | 3.22 (2.58/9.24) | 5.4 × 7.1 × 10.3 | Acidic polar | −3.50 | 147.13 | | 3.22 | 1.14 |
| Asp | 2.77 (2.07/8.18) | 8.9 × 6.9 × 5.1 | | −3.50 | 132.12 | | 10.35 | 1.12 |
| Mnz | 2.62 | 10.0 × 7.3 × 4.0 | Acidic polar | −0.02 | 171.15 | 9 | — | — |
| Cpl | 11.03 | 14.5 × 8.9 × 6.1 | | 1.14 | 323.13 | | 2.44 | 1.32 |
| Tet | 3.30 | 14.8 × 10.3 × 8.8 | | 3.00 | 480.90 | | 2.38 | 1.16 |
| Ctc | 3.30 | 14.7 × 9.5 × 7.7 | | 1.94 | 497.33 | | 2.45 | 1.15 |
| MHB | 8.50 | 10.8 × 6.7 × 4.0 | Neutral polar | 1.98 | 152.15 | 9 | — | — |
| EHB | 8.35 | 12.3 × 6.9 × 4.0 | | 2.47 | 166.17 | | 7.21 | 1.52 |
| PHB | 7.91 | 13.4 × 7.0 × 4.0 | | 2.80 | 180.20 | | 8.86 | 1.41 |
| BHB | 8.50 | 14.8 × 7.1 × 4.0 | | 3.57 | 194.23 | | 6.22 | 1.25 |
| SM1 | 2.17 | 11.9 × 9.0 × 7.1 | Amphoteric polar | — | 264.30 | 9 | — | — |
| SDM | 2.04 | 13.5 × 9.4 × 7.0 | | — | 310.30 | | 3.68 | 1.23 |
| SM2 | 2.01 | 12.8 × 9.1 × 7.6 | | — | 278.33 | | 6.69 | 1.16 |
| ST | 7.20 | 11.6 × 8.5 × 5.9 | | — | 255.32 | | 3.79 | 1.18 |
| SIZ | 1.95 | 11.3 × 9.9 × 6.1 | | — | 267.30 | | 2.99 | 1.12 |
| SMZ | 1.97 | 11.0 × 9.1 × 6.3 | | — | 253.28 | | 4.04 | 1.11 |

[a] Molecular volume (Å$^3$) from Chemdraw 3D 20.0.

Ctc maybe due to the more hydroxyl groups and the strong polarity of the chlorine element (Cl) on Ctc, which have stronger hydrogen bonds and n–π interaction with the stationary phase.[36]

For the neutral preservatives, because the effective electrophoretic mobility gradually decreased with the increased length of the alkyl chain and the dipole–dipole interaction between the preservatives and the stationary phase gradually strengthened with the increasing molecular mass and/or Log $P$ in the order MHB < EHB < PHB < and BHB (Table 2), their migration order was MHB < EHB < PHB < BHB (Fig. 10C).

The baseline separation of 6 amphoteric sulfonamides was successfully realized in a very short migration time interval (2.37 min), which was because they had the same aniline and sulfanilamide groups. Their efficient separation mainly depended on the differences of the various interactions between the substituted heterocyclic moieties, including pyridyl-, pyrimidyl-, thiazolyl-, isoxazolyl-, and the stationary phase. Generally, the migration times of the analytes with a five-membered heterocyclic ring were longer than those of the ones with a six-membered ring, which might be due to the π-bonds formed between the former and because the benzene ring of the ligands from TpBD and UiO-66-$NH_2$ in the stationary phase were stronger.[37] Among the analytes with a five-membered heterocyclic ring (SM1, SDM and SM2), because of more N, O atoms with strong electronegativity in the SDM and SM2 molecules, they easily formed more and stronger hydrogen bonds with –$NH_2$, –OH, and –COOH from TpBD and/or UiO-66-$NH_2$ in the stationary phase, resulting in the elution of both after SM1. However, the longer migration time of SM2 than SDM was due to a molecular sieve and/or stereo-hindrance effect from the larger size of –O–$CH_3$ than –$CH_3$-substituted in the pyrimidine ring. The same mechanisms were also applicable to the sulfonamides with a six-membered ring. Therefore, the migration order of the sulfonamides was SM1, SDM, SM2, ST, SIZ and SMZ (Fig. 10D).

To evaluate the separation performances of the TpBD/UiO-66-$NH_2$-bonded OT-CEC column, three families of the analytes were also separated with the TpBD- and UiO-66-$NH_2$-bonded OT-CEC column under the same experimental conditions (Fig. S11 and Table S4†). The results indicated that all the analytes achieved base-line separation in the TpBD/UiO-66-$NH_2$-bonded OT-CEC column and the TpBD-bonded OT-CEC column, but only the neutral preservatives (MHB, EHB, PHB, and BHB) were partly separated in the UiO-66-$NH_2$-bonded OT-CEC column. It could be seen that TpBD in the stationary phase of the TpBD/UiO-66-$NH_2$-bonded OT-CEC column played a dominant role in the separation of the analytes. Although the TpBD-bonded OT-CEC column had excellent separation performance for all the analytes, a significant decrease in the analysis time for the acidic antibiotics (from 6.87 min to 6.43 min) and the amphoteric sulfonamides (from 5.88 min to 4.38

Table 3 A comparison of the present work with the previous works[a]

| COF or MOF in stationary phase | Separation methods | Analyte types (numbers) | Analysis time (min) | $R_s$ | Separation system | Ref. |
|---|---|---|---|---|---|---|
| TpBD (COF) | OT-CEC | Alkylbenzenes (5), parabens (4), sulfonamides (6), benzoic acids (4) | 4.5–6.1 | 2.79–9.30 | Phosphate buffer | 33 |
| UiO-66-$NH_2$ (MOF) | OT-CEC | Chlorobenzenes (3), phenoxyacids (3), nitrophenols (3), other phenols (3) | 4.8–6.0 | — | Tris–HCl, borax buffer, citrate buffer + methanol | 38 |
| UiO-66-$NH_2$ (MOF) | IMER-CEC[a] | Chlorobenzenes (3), alkaloids (3), nonsteroidal anti-inflammatory drugs (3) | 8.5–17.6 | — | Phosphate buffer (or + acetonitrile) | 39 |
| NHP-UiO-66 (MOF) | HPLC | Substituted benzenes (5), chlorobenzenes (3), polycyclic aromatic hydrocarbons (5), nucleosides (4), polypeptides (4), proteins (4) | 8.8–14.0 | 1.54–12.28 | Phosphate buffer + acetonitrile | 40 |
| TpBD/UiO-66-$NH_2$ (MOF/COF) | OT-CEC | Amino acids (13), parabens (4), sulfonamides (6), acidic antibiotics (4) | 4.38–8.1 | 1.63–10.35 | Acetate buffer | This work |

[a] IMER is represented by immobilized enzyme micro reactor.

min) as well as a great increase in the resolutions (more than 2-fold) for the neutral preservatives were observed in the TpBD/UiO-66-$NH_2$-bonded OT-CEC column. It was obvious that UiO-66-$NH_2$ in the stationary phase enhanced the separation efficiency of the TpBD/UiO-66-$NH_2$-bonded OT-CEC column. Compared with UiO-66-$NH_2$- and/or TpBD-bonded OT-CEC column, the as-prepared hybrid OT-CEC column in this work has superior separation ability and broader application.

### 3.7 Comparison with previous studies

There are only a small number of studies on MOF or COF used as the chromatographic stationary phases and even fewer are applied for CEC. In this study, the TpBD/UiO-66-$NH_2$-bonded OT-CEC column with micro–mesoporous structures was prepared and exhibits universality for the analytes' types and properties. This is the first report on the construction of a MOF/COF hybrid material for the separation of many kinds of complex emerging pollutants by CEC. A total of 4 articles regarding OT-CEC were collected from Web of Science by searching the keywords "TpBD" or "UiO-66" and "stationary phase". As shown in Table 3, certain separation performances of the OT-CEC column prepared in this work were comparable to those reported like $R_s$ and analyte types; meanwhile, those of the others were superior. The separation performances of TpBD and/or UiO-66-$NH_2$-bonded OT-CEC column were compared in detail with the TpBD/UiO-66-$NH_2$-bonded OT-CEC column. In this work, 6 amphoteric sulfonamides realized fast baseline separation within 4.38 min, which was faster than the TpBD-bonded OT-CEC column (approaching 8.0 min). The $R_s$ of the same families of analytes (like preservatives and sulfonamides) obtained on the TpBD/UiO-66-$NH_2$-bonded OT-CEC column were all more than those on the TpBD bonded OT-CEC column. A total of 13 amino acids (acidic, neutral and basic) were simultaneously separated under broad experimental conditions. However, at most only 6 and 3 analytes were separated by the TpBD and UiO-66-$NH_2$-bonded OT-CEC columns, respectively. Furthermore, the harsh separation conditions were necessary, for example, three kinds of separation medium (Tris–HCl, borax, citrate) were applied for the separation of the target analytes by the UiO-66-$NH_2$-bonded OT-CEC column.[38] Only ammonium acetate buffer as the separation medium was simple and environment-friendly in this work. Thus, the application of the MOF/COF hybrid material in the separation field is very effective and has a good application prospect, which is especially suitable for the separation and analysis of different analytes.

## 4 Conclusions

In summary, we firstly reported an MOF/COF hybrid material (TpBD/UiO-66-$NH_2$) as the stationary phase for the separation of emerging pollutant mixtures by OT-CEC. The TpBD/UiO-66-$NH_2$-bonded OT-CEC column showed excellent separation performance for the analytes investigated including 13 amino acids, 4 antibiotics, 4 preservatives and 6 sulfonamides. All analytes achieved baseline separation within 8.1 min due to the synergistic effect between COF and MOF. The separation mechanism was primarily attributed to the combined action of hydrogen bonding, π–π interaction, molecular sieve effect, electrophoretic mobility, dipole–dipole interaction, and so on between the analytes and the stationary phase. Besides, the OT-CEC column had good stability and reproducibility with RSDs of migration time and the resolutions in the range of 1.17–3.93% and 1.79–4.31%, respectively. These results demonstrate the feasibility of introducing MOF/COF into the chromatographic column for the separation of a complex sample system, although the TpBD/UiO-66-$NH_2$-bonded OT-CEC column preparation was tedious and time consuming. In the future, more

MOF/COF in CEC separation will be established for the separation of different families of analytes, especially focusing on the applicability to real samples.

## Ethical statement

This article does not contain any studies with human or animal subjects.

## Data availability

The data supporting this article have been included as part of the ESI.†

## Author contributions

Lidi Gao: conceptualization, supervision, project administration, funding acquisition, writing – original draft, writing – review & editing. Xinran Qu: conceptualization, investigation, methodology, formal analysis, data curation, visualization, validation, writing – original draft. Shuang Meng: investigation, validation, visualization. Mo Chen: investigation, visualization. Yuxin He: investigation, visualization. Fuquan Zhao: investigation, visualization. Hongtao Chu: investigation, visualization. Shili Qin: investigation, methodology, supervision. Fenglong Jin: conceptualization, methodology, supervision.

## Conflicts of interest

The authors declare no competing interests.

## Acknowledgements

We gratefully acknowledge the support of Fundamental Research Funds in Heilongjiang Provincial Universities in 2022 (No. 145209501), Qiqihar University Graduate Innovation Project Foundation in 2022 (No. YJSCX2022002) and Qiqihar University College Students' Innovation and Entrepreneurship Training Program Funded Project in 2023 (No. x202310232003).

## References

1 G. Karina, E. Sofía, G. Rafael, A. Mariel, M. Georgia, P. Lizeth, E. Juan, M. Hafiz and P. Roberto, *MethodsX*, 2023, **10**, 102160.
2 P. Chaturvedi, P. Shukla, B. S. Giri, P. Chowdhary, R. Chandra, P. Gupta and A. Pandey, *Environ. Res.*, 2021, **194**, 110664.
3 X. Zhao, Y. Zheng, S. Y. Hu, W. H. Qiu, J. P. Jiang, C. Z. Gao, J. Z. Xiong, H. Y. Lu and F. Quan, *J. Hazard. Mater.*, 2021, **411**, 125047.
4 N. F. Zhu, K. J. Yuan, D. H. Xiong, F. X. Ai, K. Zeng, B. Y. Zhao, Z. Zhang and H. J. Zhao, *Chem. Eng. J.*, 2023, **462**, 142129.
5 C. Wang, D. Zhu, J. Zhang and Y. X. Du, *Pharm. Biomed.*, 2022, **215**, 114777.
6 V. K. Vashistha, S. Sethi, A. Mittal, D. K. Das, R. Pullabhotla, R. Bala and S. Yadav, *Environ. Monit. Assess.*, 2024, **196**, 153.
7 G. Gübitz and M. G. Schmid, *Electrophoresis*, 2004, **25**, 3981–3996.
8 X. Wang, X. Y. Hu, Y. T. Shao, L. Peng, Q. Q. Zhang, T. H. Zhou, Y. H. Xiang and N. S. Ye, *Microchim. Acta*, 2019, **18**, 1–8.
9 Z. X. Fei, M. Zhang, J. H. Zhang and L. M. Yuan, *Anal. Chim. Acta*, 2014, **830**, 49–55.
10 L. Feng, K. Y. Wang, G. S. Day, M. R. Ryder and H. C. Zhou, *Chem. Rev.*, 2020, **120**, 13087–13133.
11 C. Caratelli, J. Hajek, F. G. Cirujano, M. Waroquier, F. Xamena and V. Van Speybroeck, *J. Catal.*, 2017, **352**, 401–414.
12 F. Haase and B. V. Lotsch, *Chem. Soc. Rev.*, 2020, **49**, 8469–8500.
13 Y. Deng, Y. Wang, X. Xiao, B. J. Saucedo, Z. J. Zhu, M. S. Xie, X. R. Xu, K. Yao, Y. L. Zhai, Z. Zhang and J. Chen, *Small*, 2022, **18**, 2202928.
14 X. H. Ma, J. S. Kang, Y. W. Wu, C. H. Pang, S. H. Li, J. P. Li, Y. H. Xiong, J. H. Luo, M. Y. Wang and Z. Xu, *TrAC, Trends Anal. Chem.*, 2022, **157**, 116793.
15 J. R. Fu, S. Das, G. L. Xing, T. Ben, V. Valtchev and S. L. Qiu, *J. Am. Chem. Soc.*, 2016, **138**, 7673–7680.
16 X. L. Xu, N. Zhang, Y. Gao, T. Bao and S. C. Wang, *J. Environ. Chem. Eng.*, 2022, **10**, 107072.
17 N. Zhang, T. Bao, Y. Gao, X. L. Xu and S. C. Wang, *Appl. Surf. Sci.*, 2022, **580**, 152285.
18 J. Pang, W. J. Chen, J. T. Hu, J. Cheng, M. Q. Tang, Z. W. Liu and R. Tan, *Catal. Sci. Technol.*, 2023, **13**, 6198–6210.
19 Q. D. Yu, Y. P. Wu, W. M. Zhang, W. D. Ma, J. Wang, H. Chen, Q. Q. Ding and L. Zhang, *Talanta*, 2022, **243**, 123380.
20 L. D. Gao, X. Zhao, S. L. Qin, Q. Dong, X. F. Hu and H. T. Chu, *Chirality*, 2022, **34**, 537–549.
21 X. Q. Zhang, Q. Han and M. Y. Ding, *RSC Adv.*, 2015, **5**, 1043–1050.
22 I. Pakamore, J. Rousseau, C. Rousseau, E. Monflier and P. A. Szilágyi, *Green Chem.*, 2018, **20**, 5292–5298.
23 G. Lu, C. L. Cui, W. N. Zhang, Y. Y. Liu and F. W. Huo, *Chem.–Asian J.*, 2013, **8**, 69–72.
24 B. P. Biswal, S. Chandra, S. Kandambeth, B. Lukose, T. Heine and R. Banerjeet, *J. Am. Chem. Soc.*, 2013, **135**, 5328–5331.
25 Y. Cao, H. M. Zhang, F. J. Song, T. Huang, J. Y. Ji, Q. Zhong, W. Chu and Q. Xu, *Materials*, 2018, **11**, 589.
26 P. Khandel, S. K. Shahi, D. K. Soni, R. K. Yadaw and L. Kanwar, *Nano Convergence*, 2018, **5**, 1–17.
27 A. Khatri and P. S. Rana, *Bull. Mater. Sci.*, 2019, **42**, 141.
28 Z. H. Li, M. Q. Yang, X. T. Shen, H. T. Zhu and B. H. Li, *Int. J. Environ. Res. Public Health*, 2023, **20**, 1393.
29 G. D. Fan, J. J. Zhan, J. Luo, J. Y. Lin, F. S. Qu, B. H. Du, Y. F. You and Z. S. Yan, *J. Hazard. Mater.*, 2021, **404**, 124062.
30 S. F. Du, K. J. Lin, S. K. Malladi, Y. X. Lu, S. H. Sun and Q. Xu, *Sci. Rep.*, 2014, **4**, 6439.
31 P. Deria, W. Bury, J. T. Hupp and O. K. Farha, *Chem. Commun.*, 2014, **50**, 1965–1968.
32 H. Zhang, X. B. Shi, J. L. Li, P. Kumar and B. Liu, *Nanomaterials*, 2019, **9**, 1283.
33 L. D. Gao, Q. Dong, X. Zhao, X. F. Hu, H. T. Chu, R. J. Lv and S. L. Qin, *Processes*, 2022, **10**, 843.

34 M. Taddei, P. V. Dau, S. M. Cohen, M. Ranocchiari, J. A. van Bokhoven, F. Costantino, S. Sabatini and R. Vivani, *Dalton Trans.*, 2015, **44**, 14019–14026.
35 W. T. Li, Z. J. Hu, J. Meng, X. Zhang, W. Gao, M. L. Chen and J. H. Wang, *J. Hazard. Mater.*, 2021, **411**, 125021.
36 S. P. Gao, B. Q. Xu, X. Y. Zheng, X. Wan, X. L. Zhang, G. M. Wu and Z. Y. Cong, *Atmos. Res.*, 2021, **256**, 105597.
37 J. Hou, J. Yan, F. S. Zhang, Q. Zhao, H. Y. Chen, Y. Q. Zhang, G. J. Li, Y. Li and L. Ding, *Food Chem.*, 2014, **150**, 58–64.
38 P. X. Tang, R. Wang and Z. L. Chen, *Electrophoresis*, 2018, **39**, 2619–2625.
39 R. Liu, G. Y. Yi, B. A. Ji, X. Q. Liu, Y. Q. Gu, Z. N. Xia and Q. F. Fu, *Anal. Chem.*, 2022, **94**, 6540–6547.
40 B. A. Ji, G. Y. Yi, K. L. Zhang, Y. H. Zhang, Y. Q. Gui, D. Gao, J. Zeng, L. J. Wang, Z. N. Xia and Q. F. Fu, *Anal. Chem.*, 2020, **92**, 15655–15662.